bioRxiv preprint first posted online Mar. 31, 2018; doi: http://dx.doi.org/10.1101/292029. The copyright holder for this preprint (which was not peer-reviewed) is the author/funder, who has granted bioRxiv a license to display the preprint in perpetuity. It is made available under a CC-BY-NC-ND 4.0 International license.

Endogenous miRNA sponges mediate the generation of oscillatory dynamics for a non-coding RNA network

Andrew Dhawan[1], **Adrian L. Harris**[1], **Francesca M. Buffa**[1], **Jacob G. Scott**[2]

***For correspondence:**
scottj10@ccf.org (JGS);
adhawan@qmed.ca (AD)

[1]Department of Oncology, University of Oxford, Oxford, United Kingdom; [2]Departments of Translational Hematology and Oncology Research, Cleveland Clinic, Cleveland, United States

Oscillations are crucial to the sustenance of living organisms, across a wide variety of biological processes. In eukaryotes, oscillatory dynamics are thought to arise from interactions at the protein and RNA levels; however, the role of non-coding RNA in regulating these dynamics remains understudied. In this work, using a mathematical model, we show how non-coding RNA acting as miRNA sponges in a conserved miRNA - transcription factor feedback motif, can give rise to oscillatory behaviour. Control of these non-coding RNA can dynamically create oscillations or stability, and we show how this behaviour predisposes to oscillations in the stochastic limit. These results point towards novel hypotheses for the roles of different species of miRNA sponges, and help to provide a paradigm for functional differences between the many distinct RNA species thought to act as miRNA sponges in nature.

Oscillations are intrinsic to the behaviour of biological systems, across scales, species, stages of development, and in health and disease ***Glass*** (***2001***); ***Winfree*** (***1967***); ***Mirollo and Strogatz*** (***1990***). For example, during organismal development, oscillations are crucial to the generation of vertebrae, in a process termed somitogenesis ***Wahl et al.*** (***2007***); ***Serth et al.*** (***2003***); ***Dale et al.*** (***2006***). During this stage of development, embryonic cells entrain synchronised oscillations, resulting in the development of vertebrae in a coordinated, clock-like process. In organisms exhibiting circadian rhythms, synchronised patterns of neurotransmitter and neurohormonal release are coupled to oscillatory modes ***Welsh et al.*** (***1995***); ***Goldbeter*** (***2002***); ***Strogatz*** (***2000***). For both of these cases, a fundamental question is how a complex interacting system of biomolecules, with intrinsic stochasticity and uncertainty, is able to produce and sustain oscillatory behaviour. In somitogenesis, a seminal work in mathematical biology has proposed the 'clock and wavefront' model, which predicts the occurrence of oscillations arising from a biochemical network and diffusive effects ***Baker et al.*** (***2006***). For circadian oscillators, the discovery of the regulation of the Period protein and intercellular coupling has shown how oscillations can emerge ***Mirollo and Strogatz*** (***1990***); ***Goldbeter*** (***2002***); ***Strogatz*** (***2000***). Thus, oscillatory behaviour arises in these systems from carefully balanced interactions at the RNA and protein level, among species with specific kinetic properties, giving rise to tunable, dynamic oscillations, even in a noisy biological environment.

The manner in which the various species of non-coding RNA (ncRNA) affect these oscillatory dynamics is to be determined, as predicted functions remain elusive for circular RNA (circRNA), long non-coding RNA (lncRNA), and pseudogenes ***Li et al.*** (***2013***); ***Thomson and Dinger*** (***2016***); ***Paraskevopoulou et al.*** (***2012***); ***Jeggari et al.*** (***2012***). One common trait among each of these ncRNA is thought to be the competitive binding of miRNA, repressing these so that they are unable to

bioRxiv preprint first posted online Mar. 31, 2018; doi: http://dx.doi.org/10.1101/292029. The copyright holder for this preprint (which was not peer-reviewed) is the author/funder, who has granted bioRxiv a license to display the preprint in perpetuity. It is made available under a CC-BY-NC-ND 4.0 International license.

bind mRNA ***Ebert and Sharp*** (***2010***). This competition for miRNA binding is termed 'sponging', and is thought to be a primary function of certain circRNA, pseudogenes, expressed 3' UTRs, and potentially a function for lncRNA as well, as identified through sequence complementarity ***Thomson and Dinger*** (***2016***). In this work, we show how these ncRNA, acting as a generalised miRNA sponge on an over-represented miRNA-mRNA-transcription factor feedback motif, can give rise to sustained, tunable oscillations.

Defining a miRNA-transcription factor feedback motif

The topology of the underlying network of interactions between RNA and proteins has a direct link to the system dynamics, and understanding this has led to wider predictions about the behaviour of biomolecules in the transcriptome ***Lee et al.*** (***2002***). For instance, extending these networks to include species of non-coding RNA, such as miRNA, which act to inhibit their predicted mRNA targets, has led to understanding of their functions in fine-tuning gene expression and maintaining bistable states ***Volinia et al.*** (***2010***); ***Ryan et al.*** (***2010***); ***Li et al.*** (***2013***); ***Lai et al.*** (***2016***). These transcriptome-wide studies have shown significant over-representation of specific miRNA-mRNA-protein subnetworks, representing distinct classes of feedback and feedforward motifs, each with unique intrinsic dynamical properties ***Tsang et al.*** (***2007***). We consider an over-represented feedback motif involving a miRNA and transcription factor, as identified by Tsang et al. ***Tsang et al.*** (***2007***). This motif is seen in an interaction between the E2F transcription factor and the miR-17/92 oncogenic cluster, and we will extend this by considering the effect of a miRNA sponge, depicted graphically in Figure 1 ***Aguda et al.*** (***2008***).

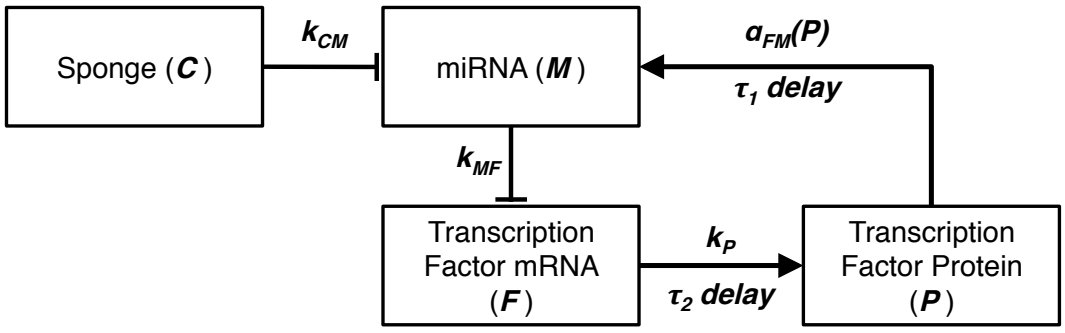

Figure 1. The miRNA sponge network considered. Directed arrows represent activation-type behaviour, and blunted arrows represent inhibitory behaviour. The system interconnections are overlayed with rate kinetic functions for each of the interactions and time delayed interactions are indicated by τ_1 and τ_2, yielding System 2.

We summarise this system mathematically by the set of equations outlined in Box 1. With this model, we analyse the long-term behaviour of this system via a stability analysis, and study the properties of the unique equilibrium solution. As per the derivation in the Supplementary Methods, we apply the Hopf bifurcation theorem to show that for cases where the time delays are non-zero, there is a Hopf bifurcation when the sum of the time delays τ_1 and τ_2 exceeds some critical time τ_0; resulting in a switch from asymptotic stability to an oscillatory steady state.

As a numerical illustration of this switch, consider the system for the following parameter values, chosen because they fall within a realistic range for known range parameters for mammalian cells as used in similar models (e.g. ***Monk*** (***2003***); ***Schwanhäusser et al.*** (***2011***)): $\alpha_C = 1$, $\delta_C = 0.01$, $\alpha_F = 1$, $\delta_F = 0.1$, $\alpha_M = 1$, $\delta_M = 1$, $k_P = 10$, $\delta_P = 0.1$, $k_{CM} = 10$, $k_{MF} = 0.1$, $\beta_{FM} = 200$, $\gamma_{FM} = 100$, and $n = 8$, with both cases of $\tau_1 = \tau_2 = 0.5$ and $\tau_1 = \tau_2 = 0.8$ as depicted in Figure 2A and B, respectively. These parameter values give a critical time τ_0 of 1.43 for which if $\tau_1 + \tau_2 > \tau_0$, there is an oscillatory solution, and when $\tau_1 + \tau_2 < \tau_0$ there is a steady state solution, as shown in Figure 2A and B.

bioRxiv preprint first posted online Mar. 31, 2018; doi: http://dx.doi.org/10.1101/292029. The copyright holder for this preprint (which was not peer-reviewed) is the author/funder, who has granted bioRxiv a license to display the preprint in perpetuity. It is made available under a CC-BY-NC-ND 4.0 International license.

Box 1. Mathematical model

Our mathematical model is defined as follows, with parameter values in Table S1. We take the concentration of sponging RNA over time t as $C(t)$, transcription factor mRNA as $F(t)$, transcription factor protein as $P(t)$, and miRNA as $M(t)$. We denote basal rates of production of sponge RNA, miRNA, and transcription factor mRNA as α_i where $i \in \{C, M, F\}$, respectively. We denote basal rates of degradation of sponge RNA, miRNA, transcription factor mRNA, and transcription factor protein as δ_i with $i \in \{C, M, F, P\}$, respectively.

Inhibitory actions between two species i and j are supposed to follow mass-action kinetics (see ***Horn and Jackson*** (***1972***) for a reference), with rate constant k_{ij} for $(i, j) \in \{(C, M), (M, F)\}$ in the case of miRNA sponge repressing miRNA and miRNA repressing transcription factor mRNA, respectively.

We suppose that the rate of production of protein from mRNA for transcription follows a delayed linear relationship to the amount of mRNA, with an average translation rate of k_P per unit of mRNA. We represent time delays by τ_1 and τ_2 in this system to account for the transcription factor-mediated activation of transcription, and translation of mRNA into protein, respectively.

The interaction term between the transcription factor and its back-activation of miRNA production is defined by the following Hill function, as in similar models (e.g. ***Ingalls et al.*** (***2017***)), such that:

$$\alpha_{FM}(P) = \frac{\beta_{FM}}{\left(\frac{\gamma_{FM}}{P}\right)^n + 1}. \tag{1}$$

From a first-order mass-action kinetics formulation, we obtain the delay differential equations, with all derivatives taken with respect to time t signified by $\dot{C}, \dot{M}, \dot{F}, \dot{P}$, as such:

$$\begin{aligned}
\dot{C} &= \alpha_C - \delta_C C - k_{CM} C M \\
\dot{M} &= \alpha_M - \delta_M M - k_{CM} C M - k_{MF} M F + \alpha_{FM}\left(P(t - \tau_1)\right) \\
\dot{F} &= \alpha_F - \delta_F F - k_{MF} M F \\
\dot{P} &= k_P F(t - \tau_2) - \delta_P P.
\end{aligned} \tag{2}$$

bioRxiv preprint first posted online Mar. 31, 2018; doi: http://dx.doi.org/10.1101/292029. The copyright holder for this preprint (which was not peer-reviewed) is the author/funder, who has granted bioRxiv a license to display the preprint in perpetuity. It is made available under a CC-BY-NC-ND 4.0 International license.

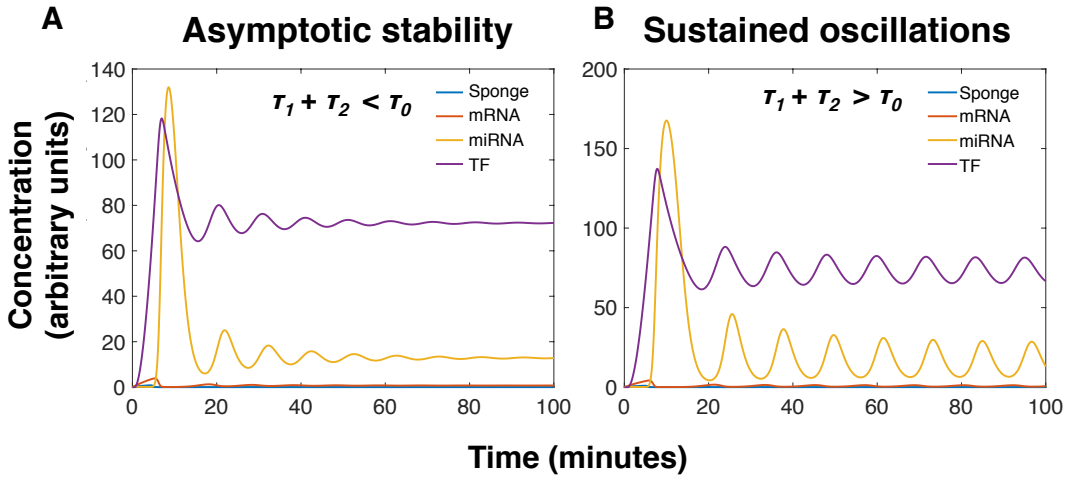

Figure 2. Increasing system delay past critical threshold induces steady oscillatory behaviour, traversing a Hopf bifurcation. Plots depict the effects of having $\tau_1 + \tau_2$ below (A) and above (B) the critical time threshold τ_0 as derived above, based on the Hopf bifurcation theorem. Common parameter values used for this simulation are: $\alpha_C = 1$, $\delta_C = 0.01$, $\alpha_F = 1$, $\delta_F = 0.1$, $\alpha_M = 1$, $\delta_M = 1$, $k_P = 10$, $\delta_P = 0.1$, $k_{CM} = 10$, $k_{MF} = 0.1$, $\beta_{FM} = 200$, $\gamma_{FM} = 100$, and $n = 8$, with τ_1 and τ_2 indicated as above.

A novel mechanism for generating sustained oscillations

Our analysis shows that there is a critical sum of the two time delays, which is is a function of system parameter values, above which oscillatory behaviour emerges. This parametric dependence of the critical time may be exploited by biological systems to generate dynamic oscillatory behaviour, as although the parameters governing the kinetics and delays present in a biological system are largely fixed, rates of production and degradation vary significantly ***Suter et al.*** (***2011***); ***Cai et al.*** (***2008***); ***Schwanhäusser et al.*** (***2011***); ***Chen et al.*** (***1999***). These may cause the system to move from an oscillatory state to a non-oscillatory state, or vice versa.

Transcriptional bursting is a phenomenon that has been observed across species for a number of genes, especially during developmental properties, whereby transcription is increased in a 'burst' over a relatively short period of time ***Suter et al.*** (***2011***). Thus, as a descriptive example, we consider a time-varying value for α_C, increasing it ten-fold from the baseline parameter values as used in Figure 2, as may occur during particular developmental processes (e.g. those in which circRNA are hypothesised to function as miRNA sponges) ***Qureshi and Mehler*** (***2012***). In this case, the new system with a parameter value of $\alpha_C = 10$ has a critical time of $\tau_0 = 0.62$, which implies that the original system with $\tau_1 = \tau_2 = 0.5$ is now oscillatory in steady state. To visualise this change, we show the system behaviour as α_C is increased ten-fold only transiently between simulation times 50 and 150 min, and is 1 otherwise, in Figure 3. Here, oscillations are created dynamically and in a time-varying fashion, with their time to disappearance primarily determined by the miRNA sponge degradation rate.

Stochastic considerations

In the case where the number of molecules is small, as may occur in single cells with low copy numbers of these biomolecules, stochastic effects will predominate. In the stochastic setting, our system is no longer described by the continuous variables written in System 2, but rather is represented by a list of events that occur at discretised time steps, which we summarise in Box 2.

Moreover, because of the presence of non-zero time delays τ_1 and τ_2, this system exhibits non-Markovian behaviour, and therefore the stochastic behaviour may not follow the mean-field approximation in the long-term. That is, there may be oscillatory behaviour in the stochastic case for a parameter regime where the deterministic model does not predict oscillations. This phenomenon,

bioRxiv preprint first posted online Mar. 31, 2018; doi: http://dx.doi.org/10.1101/292029. The copyright holder for this preprint (which was not peer-reviewed) is the author/funder, who has granted bioRxiv a license to display the preprint in perpetuity. It is made available under a CC-BY-NC-ND 4.0 International license.

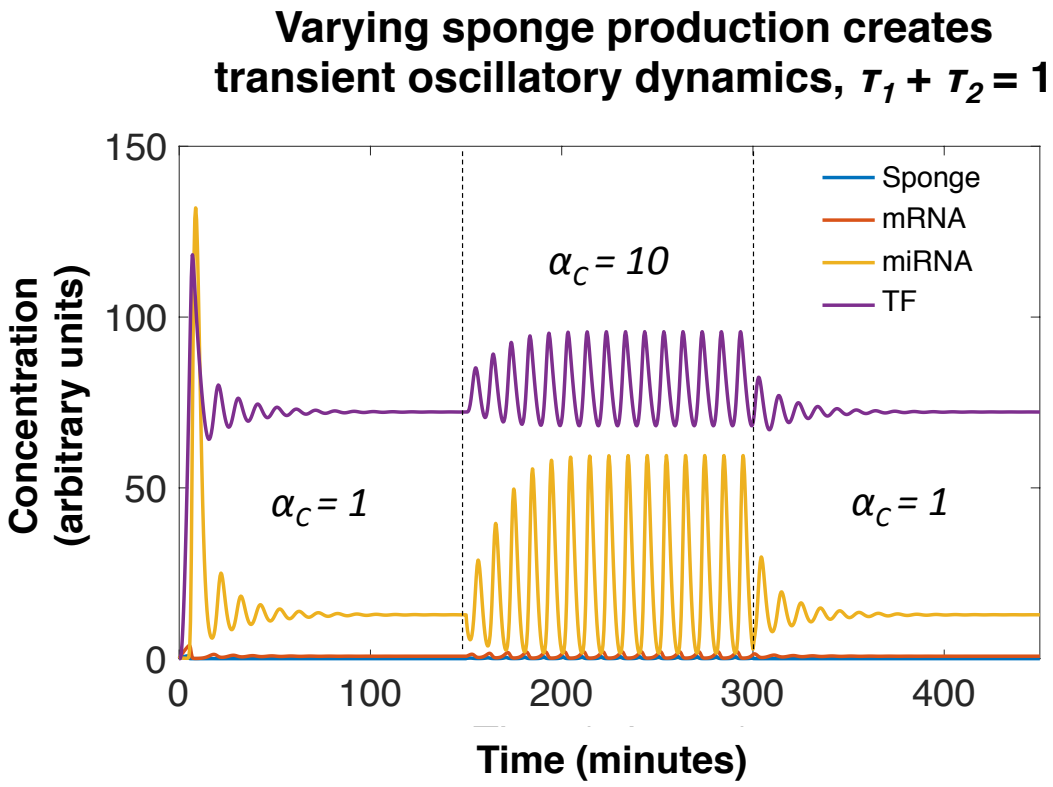

Figure 3. A time-varying α_C generates transient oscillatory behaviour. Here, a time varying value of α_C is used to illustrate the presence of a bifurcation. α_C is increased to 10 from an initial value of 1 between simulation time 150 and 300, between which oscillatory behaviour is the absorbing state, and is reduced to 1 otherwise, at which asymptotic stability predominates. Other parameter values are such that: $\delta_C = 0.01$, $\alpha_F = 1$, $\delta_F = 0.1$, $\alpha_M = 1$, $\delta_M = 1$, $k_P = 10$, $\delta_P = 0.1$, $k_{CM} = 10$, $k_{MF} = 0.1$, $\beta_{FM} = 200$, $\gamma_{FM} = 100$, and $n = 8$, with $\tau_1 = \tau_2 = 0.5$ as in Figure 2.

of *stochastic oscillations*, is one which we posit to be both significant and common among the behaviour of RNA networks, and has been thought to contribute to other oscillatory systems, such as the generation of circadian rhythms ***olde Scheper et al.*** (***1999***); ***Bratsun et al.*** (***2005***).

To capture the potential for stochastic oscillations in our system, we simulate our system numerically, noting that conventional analytic approaches to this problem are intractable as they require deriving and solving the Langevin equations derived from the reactions in System 3. The algorithm we implement, described in the Supplementary Materials (Algorithm 1) is based on the standard Gillespie algorithm, modified to handle the case of time-delayed reactions, also used for similar purposes such as delayed mRNA gene networks and chemical reaction networks ***Gillespie*** (***1977***); ***Bratsun et al.*** (***2005***); ***Anderson*** (***2007***). Briefly, in this algorithm, if a time-delayed reaction is chosen to occur based on the current state of the system, it is not executed until a future time, at which it is *scheduled* to occur, by a queuing system.

Figure 4 (left) depicts the results of a stochastic simulation for our system, showing oscillatory behaviour, with the overlayed mean field behaviour of $N = 100$ runs of the stochastic model. To study the periodicity of the stochastic signal, we take the Fourier transform of the time dynamics, and analyse the power spectra for underlying modes. Shown in Figure 4 (right), this reveals a strong subcomponent of an underlying oscillatory mode for the stochastic simulations, whereas the deterministic behaviour for this system with the same parameter values does not show this oscillatory mode.

bioRxiv preprint first posted online Mar. 31, 2018; doi: http://dx.doi.org/10.1101/292029. The copyright holder for this preprint (which was not peer-reviewed) is the author/funder, who has granted bioRxiv a license to display the preprint in perpetuity. It is made available under a CC-BY-NC-ND 4.0 International license.

Box 2. Stochastic model

The reaction 'events' and the associated rates at which they occur in the stochastic version of our system are as described in System 2, with kinetic rate parameters on the right hand side, and a time delay indicated if present for that reaction. Each of the dynamic variables and parameters is as described above and in Table S1. The symbol ∅ on the left side of a reaction indicates *de novo* synthesis, and on the right side of a reaction this indicates degradation.

$$
\begin{aligned}
\emptyset \to C &: \alpha_C & M \to \emptyset &: \delta_M M \\
C \to \emptyset &: \delta_C C & \emptyset \to P &: \alpha_P \\
\emptyset \to F &: \alpha_F & P \to \emptyset &: \delta_P P \\
F \to \emptyset &: \delta_F F & C + M \to \emptyset &: k_{CM} C M \\
\emptyset \to M &: \alpha_M & M + F \to \emptyset &: k_{MF} M F \\
\emptyset \to M &: \alpha_{FM}(P) : \tau_1 & \emptyset \to P &: k_P F : \tau_2
\end{aligned}
\tag{3}
$$

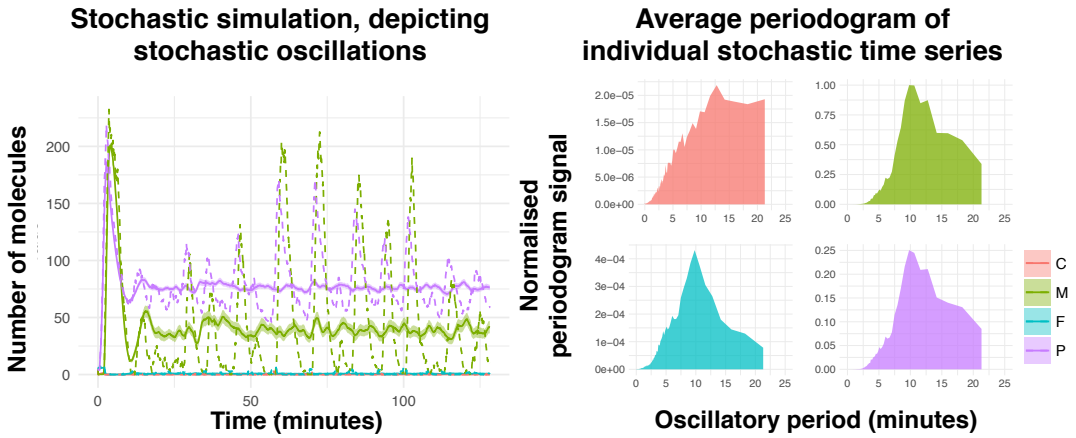

Figure 4. Stochastic system dynamics, showing an individual trace of mean behaviour and stochastic oscillations (left) and periodogram (right). Left: Averaged stochastic system dynamics do not show oscillations, but individual trajectories do. Dotted lines indicate an individual trajectory for a simulation, and bold lines are taken over an average of 100 runs, with standard error shaded around these lines.
Right: Using the dynamics from stochastic simulations, we show the presence of underlying oscillatory modes, when the mean field behaviour predicts asymptotic stability. Plots are of the average of 100 periodogram signal intensities, computed for each of the simulations of the stochastic model. Strong signal for an underlying oscillatory mode with period 10-15 minutes for the stochastic oscillations is evident, as corroborated by the individual series trace in Figure 4 (right). Parameter values used are the same as that of Figure 2, such that $\alpha_C = 1$, $\delta_C = 0.01$, $\alpha_F = 1$, $\delta_F = 0.1$, $\alpha_M = 1$, $\delta_M = 1$, $k_P = 10$, $\delta_P = 0.1$, $k_{CM} = 10$, $k_{MF} = 0.1$, $\beta_{FM} = 200$, $\gamma_{FM} = 100$, and $n = 8$, with $\tau_1 = \tau_2 = 0.5$, initial values chosen as 5 arbitrarily for all species.

Discussion

Here, we have considered a common miRNA-transcription factor network motif extended to include a miRNA sponge. We have shown how, without changing time delays or fixed kinetic parameters, oscillations can arise with simple changes in production and degradation rates of the miRNA sponge. In the stochastic case, we have shown how these oscillatory dynamics are more prevalent, and are not seen in some cases, for an equivalent set of parameters in the deterministic limit. These results have implications that show how different types of non-coding RNA acting as miRNA sponges may generate dynamics not otherwise possible in a biological system.

bioRxiv preprint first posted online Mar. 31, 2018; doi: http://dx.doi.org/10.1101/292029. The copyright holder for this preprint (which was not peer-reviewed) is the author/funder, who has granted bioRxiv a license to display the preprint in perpetuity. It is made available under a CC-BY-NC-ND 4.0 International license.

Different types of miRNA sponges confer different system behaviours

A key conclusion of this work is that different fixed kinetic properties of miRNA sponges will lead to different regimes and potentials for oscillatory dynamics in this network motif. As such, mapping these kinetic parameters to known information for the different species of RNA acting as miRNA sponges, we can hypothesise their effects, as depicted in Figure 5. For example, circRNA are differentiated from other species of ncRNA by their stability, as they do not have free ends, and so are not subject to the same RNA-se degrading enzymes ***Enuka et al.*** (***2016***); ***Gruner et al.*** (***2016***). Based on our analysis, circRNA in this network motif acting as a miRNA sponge will push the steady state closer to oscillatory behaviour, potentially crucial to the maintenance of this state. In the same vein, recent work involving circRNA characterisation has shown, through knockdown experiments, that specific circRNA are heavily involved in neurogenesis, a process where such oscillatory behaviour is likely crucial ***Piwecka et al.*** (***2017***); ***Hanan et al.*** (***2017***).

On the other hand, these results suggest that miRNA sponged by lncRNAs with a short half-life (as identified through a recent genome-wide analysis of lncRNA half-lives by Clark et al.), are likely to exhibit greater stability and less propensity towards oscillatory behaviour ***Clark et al.*** (***2012***). In effect, these lncRNA, if produced in targeted bursts, may provide tight *temporal control* of oscillatory behaviour, perhaps crucial to regulating a switch between oscillatory and non-oscillatory behaviour, as in somitogenesis.

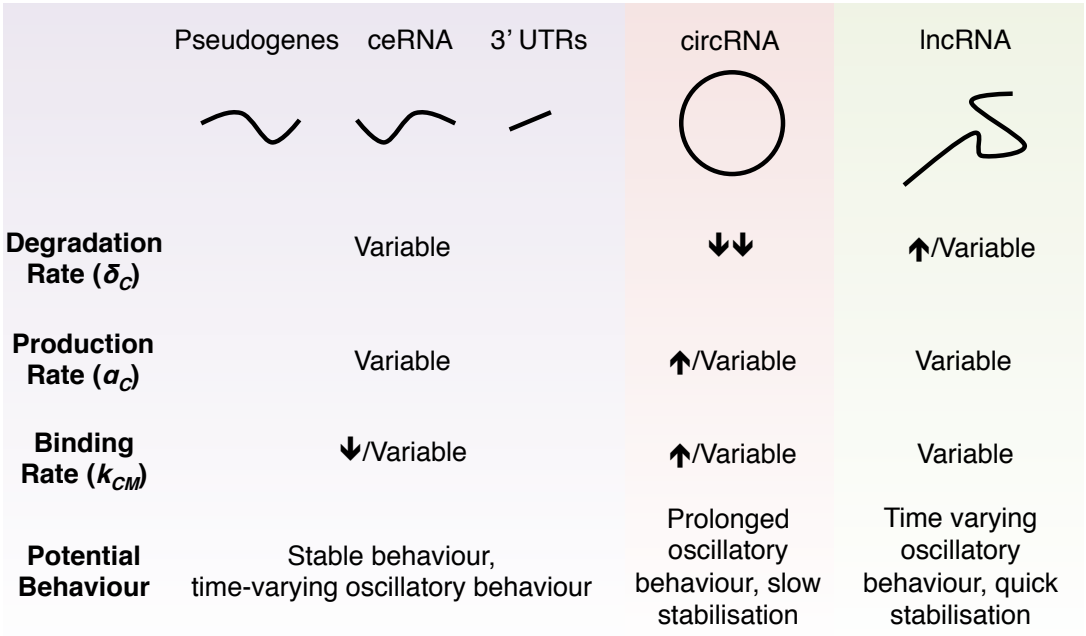

Figure 5. Summary of potential behaviours for different ncRNA acting as miRNA sponges in reaction network. Relationships between the dynamic parameters thought to occur for different ncRNA species functioning as miRNA sponges, and the effects of these parameter regimes has on system behaviour.

miRNA sponges in low copy number may be involved in the generation and maintenance of stochastic oscillations

As a result of the delay differential equation system we are considering, the system does not act in a purely Markovian manner. In practical terms, this means that the stochastic system dynamics can exhibit oscillatory behaviour, even in a parameter regime where the deterministic solution does not. This result is particularly relevant for non-coding RNA, such as circRNA, which are thought to exist with low molecular counts, suggesting that oscillatory behaviour may be a more common feature of these RNA networks than would otherwise be predicted.

bioRxiv preprint first posted online Mar. 31, 2018; doi: http://dx.doi.org/10.1101/292029. The copyright holder for this preprint (which was not peer-reviewed) is the author/funder, who has granted bioRxiv a license to display the preprint in perpetuity. It is made available under a CC-BY-NC-ND 4.0 International license.

Further, we consider the implications of extending the presented model to account for spatial differences in molecule concentration. Because the production of these biomolecules is spatially organised within the cell, and they diffuse within the nucleus and cytoplasm, the system dynamics will differ between stochastic and deterministic among various sub-regions in the cell. Regions closer to the edges of a diffusive boundary will have lower numbers of molecules, and therefore a greater propensity for stochastic oscillations, in certain cases. This may lead to a scenario in which there are steady state dynamics of the network at central regions of higher concentration, followed by disordered stochastic oscillatory behaviour as the biomolecules diffuse outward. While this level of resolution has not yet been attained experimentally, such a spatial organisation may allow cells to generate oscillations at the behaviour of a cellular membrane; potentially facilitating motile behaviour, for example.

Implications for ncRNA-based therapeutics

The results presented within this work also have implications for ncRNA-based therapeutic strategies. Figure S1 in the Supplementary Materials shows the key determinants of steady state levels for each of the species, through a parameter sensitivity analysis. Focussing on the values obtained for the system sensitivity to miRNA sponge parameters, we are able to infer the impact of a ncRNA therapeutic acting as a miRNA sponge on the network dynamics. For example, this shows that in order to decrease miRNA concentration, as opposed to increasing the binding kinetics of the sponge to the miRNA, we predict that it would be more effective to increase the production rate of the sponge (or introduce a higher concentration of miRNA sponge exogenously).

A novel experimental paradigm

This work provides fertile ground for generating hypotheses regarding the functional roles of the various miRNA sponge species. However, we have done so within the confines of the limited evidence available at the present time. Characterisation of key kinetic parameters for miRNA sponge species, through the generation of synthetic forms, could provide ample substrate for more clearly elucidating their possible dynamics. Moreover, because we predict that these miRNA sponges may lead to oscillatory behaviour, the experimental design implemented must be robust enough to capture this. Instead of supposing *a priori* that there will be asymptotically stable dynamics, multiple time points with a sufficiently fine resolution must be considered to determine whether these oscillations are present. To optimise these time points for experimental assays, guidance should be sought from a theoretical model, with an analogous analysis as presented in this work.

Overall, we have shown a novel paradigm by which oscillatory behaviour can emerge in RNA networks, via the actions of miRNA sponges. From this theoretical exploration, we have provided insight into the functional redundancy of miRNA sponges in different RNA configurations in nature. This, together with emerging knowledge of the roles of ncRNA, suggests that these species potentially have key implications for the behaviour of RNA networks in states of health and disease.

References

Aguda BD, Kim Y, Piper-Hunter MG, Friedman A, Marsh CB. MicroRNA regulation of a cancer network: consequences of the feedback loops involving miR-17-92, E2F, and Myc. Proceedings of the National Academy of Sciences. 2008; 105(50):19678–19683.

Anderson DF. A modified next reaction method for simulating chemical systems with time dependent propensities and delays. The Journal of Chemical Physics. 2007; 127(21):214107.

Baker RE, Schnell S, Maini P. A clock and wavefront mechanism for somite formation. Developmental Biology. 2006; 293(1):116–126.

Bratsun D, Volfson D, Tsimring LS, Hasty J. Delay-induced stochastic oscillations in gene regulation. Proceedings of the National Academy of Sciences of the United States of America. 2005; 102(41):14593–14598.

Cai L, Dalal CK, Elowitz MB. Frequency-modulated nuclear localization bursts coordinate gene regulation. Nature. 2008; 455(7212):485.

bioRxiv preprint first posted online Mar. 31, 2018; doi: http://dx.doi.org/10.1101/292029. The copyright holder for this preprint (which was not peer-reviewed) is the author/funder, who has granted bioRxiv a license to display the preprint in perpetuity. It is made available under a CC-BY-NC-ND 4.0 International license.

Chen T, He HL, Church GM. Modeling gene expression with differential equations. In: *Biocomputing'99* World Scientific; 1999.p. 29–40.

Clark MB, Johnston RL, Inostroza-Ponta M, Fox AH, Fortini E, Moscato P, Dinger ME, Mattick JS. Genome-wide analysis of long noncoding RNA stability. Genome Research. 2012; 22(5):885–898.

Dale JK, Malapert P, Chal J, Vilhais-Neto G, Maroto M, Johnson T, Jayasinghe S, Trainor P, Herrmann B, Pourquié O. Oscillations of the snail genes in the presomitic mesoderm coordinate segmental patterning and morphogenesis in vertebrate somitogenesis. Developmental Cell. 2006; 10(3):355–366.

Ebert MS, Sharp PA. MicroRNA sponges: progress and possibilities. RNA. 2010; 16(11):2043–2050.

Enuka Y, Lauriola M, Feldman ME, Sas-Chen A, Ulitsky I, Yarden Y. Circular RNAs are long-lived and display only minimal early alterations in response to a growth factor. Nucleic Acids Research. 2016; 44(3):1370–1383.

Gillespie DT. Exact stochastic simulation of coupled chemical reactions. The Journal of Physical Chemistry. 1977; 81(25):2340–2361.

Glass L. Synchronization and rhythmic processes in physiology. Nature. 2001; 410(6825):277–284.

Goldbeter A. Computational approaches to cellular rhythms. Nature. 2002; 420(6912):238–245.

Gruner H, Cortés-López M, Cooper DA, Bauer M, Miura P. CircRNA accumulation in the aging mouse brain. Scientific Reports. 2016; 6:38907.

Hanan M, Soreq H, Kadener S. CircRNAs in the brain. RNA Biology. 2017; 14(8):1028–1034.

Horn F, Jackson R. General mass action kinetics. Archive for Rational Mechanics and Analysis. 1972; 47(2):81–116.

Ingalls B, Mincheva M, Roussel MR. Parametric Sensitivity Analysis of Oscillatory Delay Systems with an Application to Gene Regulation. Bulletin of Mathematical Biology. 2017; p. 1–25.

Jeggari A, Marks DS, Larsson E. miRcode: a map of putative microRNA target sites in the long non-coding transcriptome. Bioinformatics. 2012; 28(15):2062–2063.

Lai X, Wolkenhauer O, Vera J. Understanding microRNA-mediated gene regulatory networks through mathematical modelling. Nucleic Acids Research. 2016; 44(13):6019–6035.

Lee TI, Rinaldi NJ, Robert F, Odom DT, Bar-Joseph Z, Gerber GK, Hannett NM, Harbison CT, Thompson CM, Simon I, et al. Transcriptional regulatory networks in Saccharomyces cerevisiae. Science. 2002; 298(5594):799–804.

Li JH, Liu S, Zhou H, Qu LH, Yang JH. starBase v2. 0: decoding miRNA-ceRNA, miRNA-ncRNA and protein–RNA interaction networks from large-scale CLIP-Seq data. Nucleic Acids Research. 2013; 42(D1):D92–D97.

Mirollo RE, Strogatz SH. Synchronization of pulse-coupled biological oscillators. SIAM Journal on Applied Mathematics. 1990; 50(6):1645–1662.

Monk NA. Oscillatory expression of Hes1, p53, and NF-κB driven by transcriptional time delays. Current Biology. 2003; 13(16):1409–1413.

Paraskevopoulou MD, Georgakilas G, Kostoulas N, Reczko M, Maragkakis M, Dalamagas TM, Hatzigeorgiou AG. DIANA-LncBase: experimentally verified and computationally predicted microRNA targets on long non-coding RNAs. Nucleic Acids Research. 2012; 41(D1):D239–D245.

Piwecka M, Glažar P, Hernandez-Miranda LR, Memczak S, Wolf SA, Rybak-Wolf A, Filipchyk A, Klironomos F, Jara CAC, Fenske P, et al. Loss of a mammalian circular RNA locus causes miRNA deregulation and affects brain function. Science. 2017; 357(6357):eaam8526.

Qureshi IA, Mehler MF. Emerging roles of non-coding RNAs in brain evolution, development, plasticity and disease. Nature Reviews Neuroscience. 2012; 13(8):528.

Ryan BM, Robles AI, Harris CC. Genetic variation in microRNA networks: the implications for cancer research. Nature Reviews Cancer. 2010; 10(6):389–402.

olde Scheper T, Klinkenberg D, Pennartz C, Van Pelt J. A mathematical model for the intracellular circadian rhythm generator. Journal of Neuroscience. 1999; 19(1):40–47.

bioRxiv preprint first posted online Mar. 31, 2018; doi: http://dx.doi.org/10.1101/292029. The copyright holder for this preprint (which was not peer-reviewed) is the author/funder, who has granted bioRxiv a license to display the preprint in perpetuity. It is made available under a CC-BY-NC-ND 4.0 International license.

288 **Schwanhäusser B**, Busse D, Li N, Dittmar G, Schuchhardt J, Wolf J, Chen W, Selbach M. Global quantification of
289 mammalian gene expression control. Nature. 2011; 473(7347):337.

290 **Serth K**, Schuster-Gossler K, Cordes R, Gossler A. Transcriptional oscillation of lunatic fringe is essential for
291 somitogenesis. Genes & Development. 2003; 17(7):912–925.

292 **Strogatz SH**. From Kuramoto to Crawford: exploring the onset of synchronization in populations of coupled
293 oscillators. Physica D: Nonlinear Phenomena. 2000; 143(1-4):1–20.

294 **Suter DM**, Molina N, Gatfield D, Schneider K, Schibler U, Naef F. Mammalian genes are transcribed with widely
295 different bursting kinetics. Science. 2011; 332(6028):472–474.

296 **Thomson DW**, Dinger ME. Endogenous microRNA sponges: evidence and controversy. Nature Reviews Genetics.
297 2016; 17(5):272–283.

298 **Tsang J**, Zhu J, van Oudenaarden A. MicroRNA-mediated feedback and feedforward loops are recurrent network
299 motifs in mammals. Molecular Cell. 2007; 26(5):753–767.

300 **Volinia S**, Galasso M, Costinean S, Tagliavini L, Gamberoni G, Drusco A, Marchesini J, Mascellani N, Sana ME,
301 Jarour RA, et al. Reprogramming of miRNA networks in cancer and leukemia. Genome Research. 2010;
302 20(5):589–599.

303 **Wahl MB**, Deng C, Lewandoski M, Pourquié O. FGF signaling acts upstream of the NOTCH and WNT sig-
304 naling pathways to control segmentation clock oscillations in mouse somitogenesis. Development. 2007;
305 134(22):4033–4041.

306 **Welsh DK**, Logothetis DE, Meister M, Reppert SM. Individual neurons dissociated from rat suprachiasmatic
307 nucleus express independently phased circadian firing rhythms. Neuron. 1995; 14(4):697–706.

308 **Winfree AT**. Biological rhythms and the behavior of populations of coupled oscillators. Journal of Theoretical
309 Biology. 1967; 16(1):15–42.